Organic & Biomolecular Chemistry

This article is part of the

OBC 10th anniversary

themed issue

All articles in this issue will be gathered together online at

www.rsc.org/OBC10

Organic & Biomolecular Chemistry

Dynamic Article Links
View Online

Cite this: *Org. Biomol. Chem.*, 2012, **10**, 6054

www.rsc.org/obc

PAPER

Vinyl-triphenylamine dyes, a new family of switchable fluorescent probes for targeted two-photon cellular imaging: from DNA to protein labeling†‡

Blaise Dumat,[a] Guillaume Bordeau,[a] Ana I. Aranda,[a] Florence Mahuteau-Betzer,[a] Yara El Harfouch,[b] Germain Metgé,[b] Fabrice Charra,[b] Céline Fiorini-Debuisschert[b] and Marie-Paule Teulade-Fichou*[a]

Received 9th March 2012, Accepted 1st May 2012
DOI: 10.1039/c2ob25515d

On the basis of our previous work on vinyl-triphenylamine derived DNA fluorophores we explored the structure space around this core by coupling it to diverse cationic, anionic and zwitterionic groups in the aim of targeting different classes of biomolecules. In parallel core modifications were performed to optimize the photophysical properties (quantum yield, two-photon absorption). The resulting water soluble π-conjugated molecules are called TP dyes and display an exceptional combination of optical properties: high two-photon absorption cross-section, high photostability, no self-quenching, and switchable fluorescence emission when bound to a biopolymer matrix. The linear and nonlinear optical properties of the TP dyes were studied *in vitro* in presence of DNA and in presence of a model protein (human serum albumin) using complementary absorption and fluorescence spectroscopy characterization tools. Structure modifications enabled to switch from DNA probes (cationic TP-pyridinium series) to protein probes (anionic TP-rhodanine series) without affecting the optical properties. Finally most TP compounds appear cell-permeant and show an intracellular localization consistent with their *in vitro* target specificity.

Introduction

Since its emergence in the nineties, two-photon laser-scanning microscopy has been shown to be a powerful technique for the study of dynamic processes and live-cell imaging.[1] The non-linear origin of the signal leads to intrinsic 3D sectioning thus preventing any out-of-focus fluorescence signal. In the meantime, infra-red (IR) excitation causes less damage to the sample than UV-Vis and yields no endogenous contribution to the fluorescence. In addition the IR range is in the optical transparency window of biological tissues thereby enabling thick sample imaging, which is otherwise difficult at shorter wavelengths due to strong absorption and diffusion in biological tissues. These features make two-photon excitation far more efficient than monophotonic excitation for live-cell imaging and even more interestingly for intravital microscopy.[2]

The low probability of occurrence of nonlinear optical phenomenon requires the use of pulsed femtosecond lasers to provide a high instantaneous photon density but with a low average energy that would be otherwise deleterious for the samples. It is also necessary to design fluorescent probes with optimized two-photon absorption (2PA) cross-sections since most of the usual dyes used in microscopy (for instance fluorescein and the DNA stainer DAPI) have particularly low 2PA cross sections (δ < 1–10 GM).[3,4] The use of optimized probes allows to maintain good image brightness and contrast while lowering the excitation power, causing less damage to the sample and less photobleaching.

Early works on nonlinear absorption of push–pull π-conjugated dipolar molecules (D-π-A) have established that increasing the internal charge transfer (and more specifically symmetric internal charge transfer) and the dimensionality of the molecule improves the two-photon absorption cross-section.[5,6] By combining synthesis and theory, this has led to the development of π-conjugated quadrupolar systems (D-π-A-π-D or A-π-D-π-A) displaying high absorption cross-sections. Subsequently octupoles formed by three symmetric dipoles have been shown to be highly efficient 2PA absorbers.[7–10] According to these guidelines, the triphenylamine core has been selected as a privileged building unit for the design of symmetric octupoles as its strong electron donor feature, its C_3 symmetry and its versatile chemistry represent major advantages. Indeed, a considerable number of triphenylamine derivatives have been successfully used in material chemistry and more recently appear

[a]*UMR 176 CNRS/Institut Curie, Institut Curie, Bât 110, Université Paris-Sud, F-91405 Orsay, France. E-mail: mp.teulade-fichou@curie.fr*
[b]*CEA-Saclay, DSM/IRAMIS/SPCSI, F-91191 Gif-sur-Yvette, France*

† This article is part of the *Organic & Biomolecular Chemistry* 10th Anniversary issue.

‡ Electronic supplementary information (ESI) available: Materials and methods, Synthesis, Complementary experiments. See DOI: 10.1039/c2ob25515d

in a number of molecular systems devoted to photovoltaic applications.[11,12] Nonetheless, such molecular engineering considerations have led to high molecular weight aromatic molecules which are *a priori* non suitable for biological imaging. Solutions exist, such as micelle encapsulation,[13,14] to address this issue and enable the use of such molecules in aqueous media, but there is still a lack of ready-to-use, low-molecular weight biological probes with optimized 2PA cross-sections.

Another important criteria rarely met when developing biofluorophores is the intrinsic direct affinity for a given type of biomolecule (DNA, RNA, proteins) or for a cellular compartment or organelles (mitochondria, lysosomes, cell-membrane *etc.*), which will enable site-specific labeling. Although cellular specificity can be achieved by conjugation to diverse chemical or biological tags (*e.g.* spermine, folate, peptides, antibodies),[15–17] this is often synthetically laborious, may affect the optical properties and *in fine* may result in highly expensive probes. Therefore spontaneous binding of high brightness dyes to a unique class of macromolecule represents a considerable advantage to assess specific localization in cells. This property is at the origin of a number of organic dyes featured in the toolbox of cell biologists for the specific staining of cell components.

In this context we launched a program aimed at developing hydrosoluble targeted two-photon excitable dyes derived from a triphenylamine (TP) core. In a first study we introduced pyridinium units on the TP core by a sequential Heck cross coupling–methylation pathway starting from the bis- or tris-bromotriphenylamine. The resulting cationic dyes TP-2Py and TP-3Py (Fig. 1) were shown to be highly efficient two-photon dyes with a specific and strong affinity for DNA.[18,19] They are virtually not fluorescent in the free state in aqueous buffer and strongly fluorescent when bound to the DNA matrix. This property of utmost importance for cellular imaging, is attributed to both the screening from water once the dye is inserted inside DNA and to the immobilization that reduces non-radiative processes associated to molecular internal rotation around the vinyl bond.[20] Based on these results, we modified both the electron-withdrawing groups and the central TP core in the aim of optimizing the photophysical properties and changed the global charge of the molecule to study the possibility of expanding the target range and applicability of the dyes. Exploration of molecular interactions of the newly prepared series with both nucleic acid matrices and a model protein (HSA) evidenced that we can switch from DNA to protein labeling with only minor alteration of the 2PA brightness (2PA cross-section δ × quantum yield Φ_F). The report is completed by cellular imaging data that corroborate the target preferences observed *in vitro*. Altogether the present results emphasize the highly versatile potential of the vinyl triphenylamine class of compounds in terms of molecular diversity and of bioimaging.

DNA probes

As mentioned above, TP-2Py and TP-3Py are fluorescent DNA off–on probes that exhibit a large fluorescence enhancement in the presence of DNA. However, this fluorescence restoration is strongly conformation dependent and is observed essentially in presence of duplex DNA and neither in the presence of single stranded DNA nor in the presence of total cellular RNA (calf liver).[18] It thus appears that the fluorescence increase is correlated to a strong binding preference for duplex DNA. However, it cannot be completely excluded that the compounds interact with other DNA or RNA forms without being fluorescent.

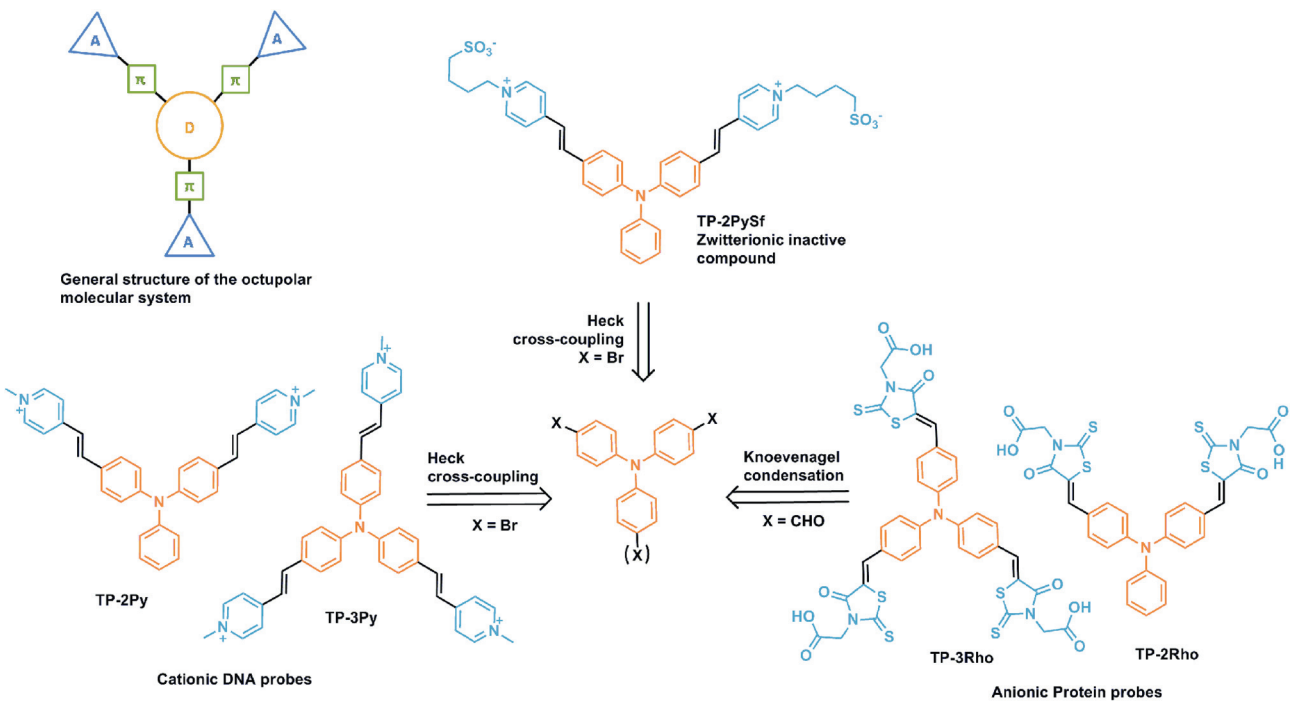

Fig. 1 Electron acceptor groups were tethered to the triphenylamine core by straight-forward and high-yielding procedures to give octupolar systems with optimized two-photon absorption cross-sections. The nature and number of those groups determines the properties of the fluorophore.

Table 1 Optical properties of the cationic dyes in glycerol and in DNA (30 equivalents in base pairs of herring testes DNA in 10 mM sodium cacodylate buffer pH 7.2, 100 mM NaCl)

	ε (mol^{-1} L cm^{-1})		Φ_F		δ (GM)	
	Glycerol	DNA	Glycerol	DNA	Glycerol	DNA
TP-2Py	37 400 (496 nm)	31 400 (509 nm)	0.11 (649 nm)	0.08 (656 nm)	390 (820 nm)	450 (820 nm)
TP-3Py	66 000 (492 nm)	51 000 (499 nm)	0.13 (666 nm)	0.01 (684 nm)	780 (820 nm)	700 (820 nm)
TP-2PySf	46 000 (498 nm)	42 100 (481 nm)	0.16 (657 nm)	n.d.	210 (820 nm)	n.d.
Cbz-2Py	28 700 (444 nm)	21 700 (451 nm)	0.33 (580 nm)	0.58 (545 nm)	190 (800 nm)	210 (800 nm)
Cbz-3Py	61 100 (437 nm)	44 200 (441 nm)	0.16 (581 nm)	0.03 (552 nm)	540 (760 nm)	320 (820 nm)
TN-3Py	62 000 (488 nm)	62 000 (493 nm)	0.05 (701 nm)	n.d.	1750 (820 nm)	n.d.

Molar absorption coefficient ε measured at the maximum absorption wavelength indicated in parenthesis, fluorescence quantum yield Φ_F with the maximum emission wavelength and two-photon absorption cross-section δ measured at the maximum two-photon absorption wavelength in parenthesis, n.d.: not determined.

In the presence of herring testes DNA, both dyes exhibit large 2PA cross-sections in the IR and confirm the advantage of the three-branched octupolar compound TP-3Py (700 GM at 820 nm) over to the two-branched quadrupolar counterpart TP-2Py (450 GM at 820 nm, Table 1),[18] in consistency with numerous works in the field.[6,7] However, if we compare the 2PA brightness ($\delta \times \Phi_F$) that is the relevant figure of merit for imaging, TP-2Py shows a significantly higher brightness than TP-3Py in DNA (35 GM *vs.* 19 GM), in contrary to values in glycerol, thereby emphasizing the necessary balance between optical and DNA binding properties.

When imaging cells *via* two-photon excited fluorescence (2PEF) microscopy, both dyes induce a bright specific staining of nuclear DNA with a red emission (λ_{max} = 656, 684 nm) and a particularly high signal to noise ratio.[18] Worth mentioning is their large Stokes shift (*ca.* 150 nm), typical of push–pull systems that display strong charge transfer during excitation (ESI‡). The TP-Py dyes are non-cytotoxic in the micromolar range (ESI‡), live cell permeant and thus perfectly suitable for cellular imaging by one and two-photon excited confocal microscopy. However, they have rather modest quantum yields and attempts have been made to increase this parameter by replacing the triphenylamine core with a more rigid carbazole core. In parallel we also increased the electron donor ability of the central core and π-conjugation by introducing a trinaphthylamine core (TN) in place of the triphenylamine (Fig. 2). This modification was expected to improve both the quantum yield and the internal charge transfer.

As previously reported, the carbazole analogues, Cbz-2Py and Cbz-3Py, fulfill the objective with a quantum yield of 0.58 in DNA for Cbz-2Py. This results in a strongly optimized 2PA brightness ($\delta \times \Phi_F$ = 121 GM), although the carbazole core causes a two-fold decrease in the 2PA cross-section (Table 1).[21] Also, the rigidification of the core induces a blue-shift of the emission (approx 100 nm) thereby causing a loss of the NIR characteristic of the TP series. According to preliminary modeling studies, the binding to DNA was likely to occur *via* insertion of the bis(arylvinylpyridinium)amine pattern in the minor groove of duplex DNA. These observations were confirmed by circular dichroism (CD) experiments performed with two different oligonucleotides, a 12-mer duplex presenting a central AAATTT site favoring minor groove binding [d(CGCGAAATTTCGCG)2, drewAT] and a 26-mer duplex displaying no particular base

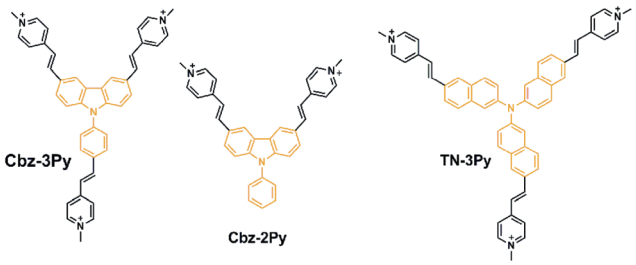

Fig. 2 Variation on the electron-donating core of the pyridinium derivatives.

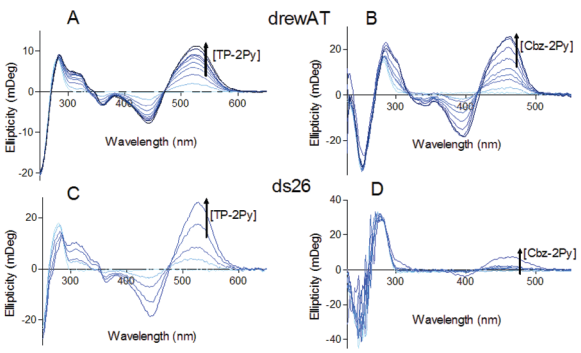

Fig. 3 Circular dichroism spectra of drewAT and ds26 upon addition of TP-2Py and Cbz-2Py. (A,C) [DNA] = 3 μM, [TP-2Py] = 0–18 μM (B,D) [DNA] = 5 μM, [Cbz-2Py] = 0–25 μM. Buffer: 10 mM sodium cacodylate pH 7.2 + 100 mM NaCl.

repeats [d(CAATCGGATCGAATTCGATCCGATTG)2, ds26]. In presence of both oligonucleotides, the triphenylamine derivatives exhibited a large induced CD signal characteristic of minor groove binding (Fig. 3). On the other hand, the carbazole derivatives only gave an induced signal in drewAT and not in ds26 except at very high dye–DNA ratios. The interaction of Cbz derivatives appears sequence-dependent whilst that of the TP compounds is not or to a much lesser extent. Modeling studies attributed this difference in behavior to a preferential binding of Cbz-2Py in the major groove of ds26.[21]

The neutral precursor of TN-3Py was synthesized according to a previously reported procedure and methylated by methyl

iodide in a dichloromethane–methanol mixture (ESI‡).[22] Although the fluorescence quantum yield of the new dye in glycerol was lowered by a factor of two compared to that of TP-3Py, a dramatic improvement of the 2PA cross section was measured (δ = 1750 GM *vs*. 780 GM for TP-3Py). Yet this compound shows almost no fluorescence enhancement in presence of herring testes DNA thereby indicating its poor ability to bind to DNA, likely due to the larger size of the trinaphthyl core.

Despite their significantly higher quantum yields, the carbazole derivatives have lower 2PA cross sections and furthermore have lost the NIR emission that is an important advantage for bioimaging. On the other hand, the trinaphthylamine displays considerably enhanced 2PA cross section but does not interact with DNA. These balanced performances of the core-modified pyridinium derivatives underline the difficulties of fluorescence engineering in optimizing both optical properties and targeting ability.

To complete the structural modifications of the pyridinium series the zwitterionic compound TP-2PySf was synthesized by reaction between the neutral pyridine intermediate with 1,4-butanesultone (ESI‡). The aim was to modify the charge without affecting the 2PA absorption capacity,[23] whilst retaining the water solubility. In glycerol, the TP-2PySf displays a quantum yield close to that of the cationic TP-2Py (Table 1). On the other hand in presence of DNA the fluorescence is not restored, thereby indicating weak DNA binding. This suggests that the net charge of the ligand is essential for the association of the two partners before the establishment of local electrostatic interactions in the binding site which will further stabilize the complex.

Based on these results, the formal charge of the dyes was completely reversed to give two anionic molecules TP-2Rho and TP-3Rho aimed at targeting new macrobiomolecules such as proteins.

Charge inversion: towards protein targeting

The two anionic dyes, TP-2Rho and TP-3Rho bearing carboxylic acid functions negatively charged at physiological pH, were obtained according to a reported procedure based on Knoevenagel condensation of rhodanine acetic acid on bis- or tris-formyltriphenylamine (ESI‡).[24] In organic media TP-2Rho and TP-3Rho behave like their cationic counterparts, displaying a bright fluorescence emission around 600 nm which is completely quenched in aqueous solution (Table 2). Yet, as expected, by reversing the charge of the probes, the affinity for nucleic acids is lost and no restoration of the fluorescence signal is observed upon addition of duplex DNA (data not shown). We then examined the interaction of the two dyes with the human serum albumin protein which was taken as model.

Albumin accounts for 60% of the total protein in blood serum. It serves as a transport protein, and, as such, binds a variety of endogenous and exogenous ligands.[25–30] In their early work in 1975, Sudlow *et al.* identified two families of anionic drugs, mostly carboxylic acids, which specifically bind to two sites called site I and II.[31,32] Other sites have been identified that bind fatty acids and metal cations, as well as multiple nonspecific secondary sites.[33] In spite of the large structural variety of the SA ligands, a few guidelines have emerged to rationalize their design: for site II ligands, the carboxylic group is located at one end of the extended aromatic structure, while site I ligands are more bulky aromatics with a central and often delocalized negative charge.[34]

With their carboxylic acid groups borne by the rhodanine extremities and the hydrophobic triphenylamine core TP-2Rho and TP-3Rho respond to the aforementioned molecular guidelines. Moreover, rhodanine is a widely used scaffold in drug design,[35] and several of its derivatives are known to inhibit proteins.[36,37] This motif can also be viewed as a sulfur analogue of the chromophores found in fluorescent proteins.[38]

Optical properties

In organic solvents. The optical properties of the dyes were first studied in dichloromethane (DCM) and glycerol (Table 2). The nature of the solvent seems to have little influence on the absorption properties. Each molecule absorbs at the same wavelength with comparable molar absorption coefficients in both media. Regarding emission, a slight solvatochromism effect is observed between dichloromethane and glycerol; the fluorescence signal is blue-shifted in dichloromethane with fluorescence quantum yield approximately twice as high compared to glycerol, showing that the fluorescence emission of the TP-Rho is polarity-dependent.

In presence of human serum albumin. The two compounds were then studied in aqueous buffer, and both exhibited high molar absorption coefficients around 70 000 mol^{-1} L cm^{-1} in the 500 nm range confirming that the absorbance of these molecules is insensitive to the environment (ESI‡). In these conditions a very low fluorescence signal was recorded which prevented fluorescence quantum yield determination. However, the strongly red-shifted emission wavelength (*i.e.* 630 nm and 680 nm for TP-2Rho and TP-3Rho respectively, data not shown) is consistent with the solvatochromism observed when shifting from dichloromethane to glycerol. Addition of the human serum

Table 2 Optical properties of TP-2Rho and TP-3Rho in dichloromethane and glycerol

	ε (mol^{-1} L cm^{-1})		Φ_F		δ (GM)	
	Dichloromethane	Glycerol	Dichloromethane	Glycerol	Dichloromethane	Glycerol
TP-2Rho	78 800 (500 nm)	76 300 (500 nm)	0.16 (600 nm)	0.09 (615 nm)	379 (870 nm)	n.d.
TP-3Rho	78 500 (490 nm)	78 200 (490 nm)	0.13 (597 nm)	0.07 (625 nm)	425 (820 nm)	n.d.

Molar absorption coefficient ε measured at the indicated maximum absorption wavelength, fluorescence quantum yield Φ_F with the maximum emission wavelength and two-photon absorption cross-section δ (GM) measured at the indicated maximum two-photon absorption wavelength.

Table 3 Optical properties of the TP-Rho in presence of human serum albumin in 10 mM sodium cacodylate buffer pH 7.2

	ε (mol^{-1} L cm^{-1})	Φ_F	δ (GM)
TP-2Rho	58 900 (500 nm)	0.028 (585 nm)	464 (870 nm)
TP-3Rho	68 900 (486 nm)	0.015 (620 nm)	773 (820 nm)

Fluorescence quantum yield Φ_F (maximum emission wavelength), molar absorption coefficient ε measured at the maximum absorption wavelength and two-photon absorption cross-section δ measured at the maximum two-photon absorption wavelength.

albumin protein (HSA) induces a slight hypochromism of the absorption, but still no significant shift of the maximum wavelength (Table 3, ESI‡). On the other hand, a large increase of the fluorescence quantum yield is measured with 5 molar equivalents of protein with a pronounced blue-shift of the emission wavelength (45 to 60 nm, Table 3 and Fig. 4A and B). These features strongly suggest binding of the molecules in the hydrophobic pockets of the protein. Indeed, the strong blue-shift in the emission wavelength correlates to a reduction of the polarity of the environment of the molecules attributable to a shielding from water. Although molecular motions should participate strongly to fluorescence quenching, both dyes were significantly more fluorescent in dichloromethane than in glycerol and in HSA. Thus TP-Rho immobilization following interaction with the protein does not seem to be solely at the origin of fluorescence restoration, which should result from more complex multiple effects (hydrophobic, electronic).

Nonlinear optical properties. 2PA cross-sections were determined in dichloromethane and in HSA (dye–HSA molar ratio 1 : 5) by a two-photon induced fluorescence method using fluorescein in water as a reference. The charge modification of the end terminal group does not affect the 2PA capacity and the TP-Rho derivatives remain efficient non-linear dyes with cross-sections around 400 GM in DCM (Table 2). In presence of HSA the 2PA spectra exhibit the same maxima as in DCM (see ESI‡). However, significantly higher cross-section values are observed, especially in the case of the TP-3Rho which has a cross-section almost twice higher than that in DCM (Table 3). As seen with the pyridinium series, the octupolar compound TP-3Rho is more efficient in terms of nonlinear absorption than its quadrupolar counterpart TP-2Rho and the difference between both compounds is much higher in HSA than in DCM.

Interaction with HSA

The formation of the HSA–dye complex was studied more thoroughly using fluorescence spectroscopy. Fluorimetric titrations with HSA showed different behaviors for TP-2Rho and TP-3Rho. For TP-2Rho, a gradual increase of fluorescence is observed until saturation at approximately four molar equivalents of HSA with a final 75-fold fluorescence enhancement (Fig. 4A). Likewise, a strong fluorescence increase is observed for TP-3Rho until approx. one equivalent of HSA but is immediately followed by a fluorescence decrease (Fig. 4B) that reaches a plateau at 4 molar equivalents of protein with a final 30-fold fluorescence enhancement. The biphasic titration curve could not be fitted either by one or two-site models revealing a complex

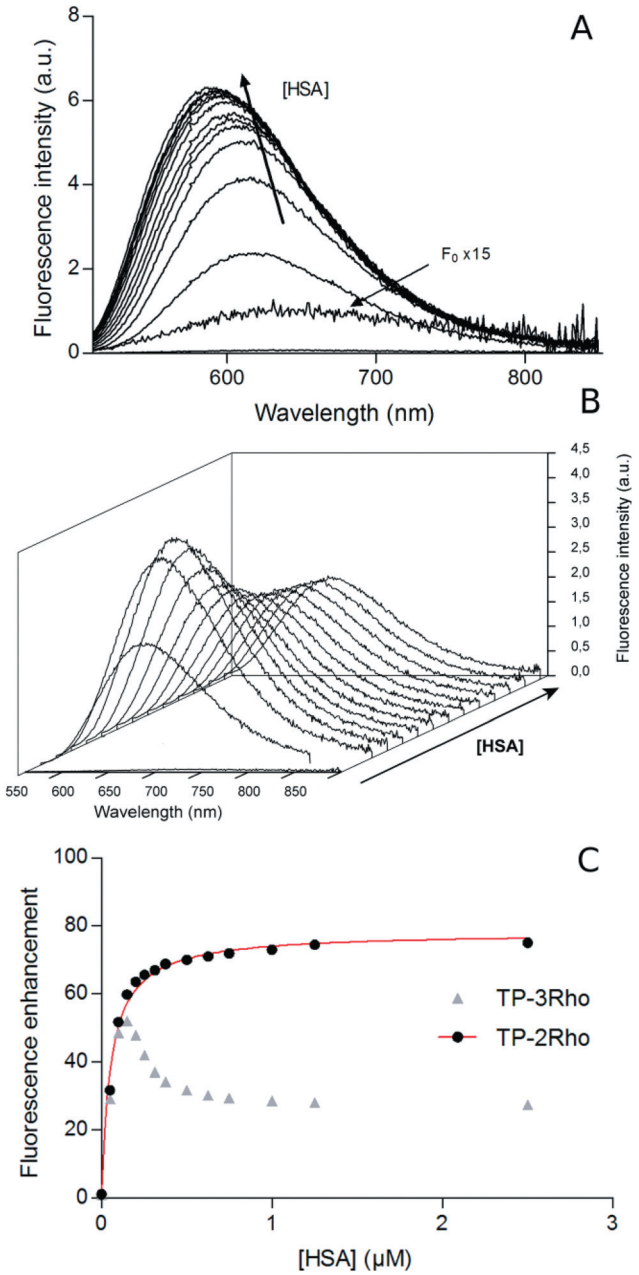

Fig. 4 Fluorimetric titrations of (A) TP-2Rho and (B) TP-3Rho by HSA. [dye] = 0.25 μM in 10 mM sodium cacodylate buffer pH 7.2. (C) Corresponding titration curves obtained by plotting the fluorescence enhancement F/F_0 *versus* the concentration in HSA, where F is the dye–protein complex fluorescence and F_0 the free dye signal.

binding event. A possible explanation is that the excess of HSA causes the relocation of the molecules to secondary sites where they are not fluorescent. On the other hand, the TP-2Rho data fit a one-site binding model with an affinity constant of 1.8×10^7 M^{-1} (ESI‡).

Competitive fluorimetric titrations – binding site

In an attempt to have insight on the binding site of the TP-2Rho dye on the human serum albumin, we used warfarin and

ibuprofen as probes since these compounds are well-known site I and II ligands respectively (ESI‡). Both TP-Rho could not be efficiently displaced by warfarin or ibuprofen indicating the higher affinity of the dyes for the serum albumin proteins. However drug–HSA interactions can also be studied by following the fluorescence variation of warfarin upon competitive displacement.[39] In our case it appeared possible to record simultaneously the fluorescence increase of the TP dyes upon competitive binding (Fig. 5).

The fluorescence of warfarin in HSA is almost completely quenched upon addition of TP-2Rho or TP-3Rho thus indicating strong displacement of the drug by the two dyes. The fluorescence quenching of warfarin correlates with the increase of the TP-2Rho signal with curves crossing at 1 μM of added TP-Rho (*i.e.* 50% of the starting warfarin concentration) with 50% of relative increase in TP-Rho fluorescence intensity indicating that half of the drug is displaced by an equivalent molar concentration of dye. This observation is consistent with the 1 : 1 binding process previously shown. These data indicate that TP-2Rho predominantly forms a 1 : 1 complex in the site I of HSA with a high affinity constant. Again the warfarin displacement curve obtained for the TP-3Rho/HSA is less well-defined but globally the displacement remains rather efficient, indicating that TP-3Rho also interact with the protein site I, although the interaction is more complex and multiple than that of its two-branch counterpart. Indeed the additional charge and the more sterically hindered propeller shape of the three-branched compound is likely to induce more complex interactions and more difficulties for fitting tightly into binding pockets.

It thus appears that the two-branched compound is the best compromise for a structure specific probe with optimized two-photon cross-section for DNA as well as for protein labeling.

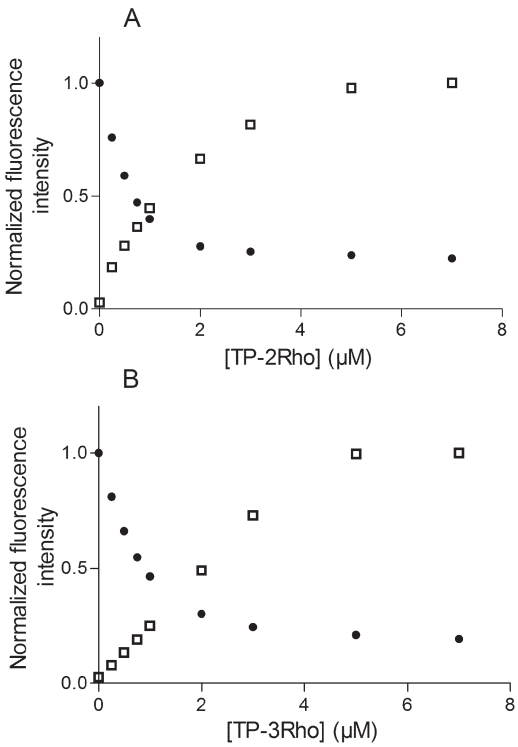

Fig. 5 Competitive displacement of warfarin by TP-2Rho (A) and TP-3Rho (B) in HSA monitored by fluorescence (Exc 320 nm). Emission: 340–500 nm (warfarin) 500–600 nm (TP-Rho). [HSA] = [warfarin] = 2 μM in 10 mM sodium cacodylate buffer. Normalized fluorescence intensity of warfarin (squares) and TP-Rho (circles) plotted *versus* the concentration of competitor.

Cellular imaging by confocal and 2PEF microscopy

The dyes were tested in cells by confocal microscopy. After incubation of live cells for two hours with dyes at 2 μM, cells were washed before fixation with PFA. In these conditions and as previously reported, TP-2Py and Cbz-2Py show a very bright staining of DNA under two-photon excitation with very low fluorescence background in the cytoplasm (Fig. 6 and 7B). Although the cellular distribution can be modified by the fixation protocol, this experiment proves at least that the dyes are

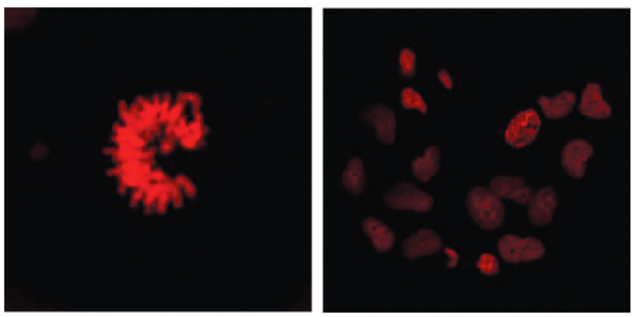

Fig. 6 Fixed MRC-5 cells stained by TP-2Py under two-photon excitation (λ_{exc} = 820 nm).

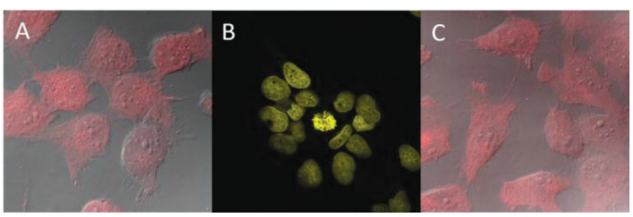

Fig. 7 Fixed MRC-5 cells stained by TP-2PySf (A), Cbz-2Py (B) and TN-3Py (C) under one (A,C) and two-photon (B) excitation.

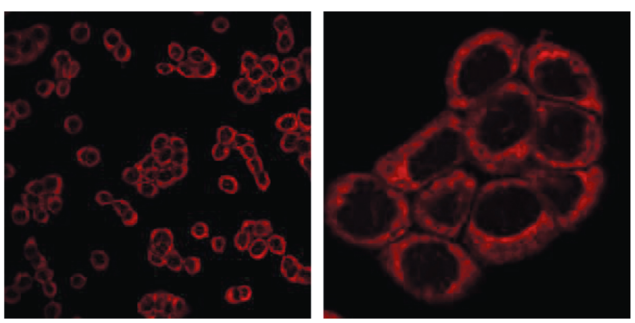

Fig. 8 Fixed HT29 cells stained by TP-2Rho under two-photon excitation (λ_{exc} = 800 nm).

live cell permeant. In correlation to their absence of interaction with RNA observed *in vitro*, no fluorescence is observed in the nucleoli or in the cytoplasm unlike DNA stainers such as PI or TOTO3 that require RNAse treatment before imaging.[40] The dyes were also found to be highly photostable compared to usual DNA stainers such as TO-PRO3.[18]

TN-3Py and TP-2Pysf exhibit a faint and diffuse staining of the whole cell (Fig. 7A and 7C) which correlates with the absence of DNA affinity observed *in vitro*.

Finally and as expected the TP-2Rho dye does not induce nuclear DNA staining. However, bright fluorescent spots in the cytoplasm show that the dye stains specific organelles the identification of which will be investigated in the future (Fig. 8). Cytoxicity evaluated on two cell lines indicate that the TP-Rho series has a very low cytoxicity (ESI‡).

Conclusion

Starting from a series of light up DNA probes based on a vinyltriphenylamine scaffold (TP-Py) we made structural modifications in order to improve their one and two-photon optical properties and enlarge the repertoire of their biomolecular target specificity.

In the case of pyridinium end groups, we have shown that both fluorescence quantum yield efficiency and two-photon absorption cross-section can be significantly enhanced by rigidifying the structure of the donor core (Cbz-Py), or by increasing its size and electron richness (TN-Py). Although in the latter case the structural modification is made at the expense of the DNA target affinity.

On the other hand, replacement of the pyridinium end group by the rhodanine motif bearing a carboxylic function (TP-Rho) enabled switching from DNA to protein binding while keeping the light up property and without affecting significantly the 2PA capacity. Although HSA is a model protein, our results suggest that the obtained rhodanine derivatives have potential for labeling other class of proteins present in subcellular structures.

Although the three-branched TP scaffold is theoretically more efficient for two-photon absorption, the two-branched derivatives seem to have more well-defined binding interaction with targets (both DNA and HSA). Thus the two-branched scaffold represents the best compromise between optical properties and target specificity.

In conclusion, we demonstrated herein that the vinyltriphenylamine motif is a powerful scaffold for the development of a large variety of compounds through high-yielding one or two-step synthetic procedures. The resulting TP-dyes represent a new family of switchable biolabels that display essential criteria for single and two-photon excitation fluorescence imaging in cells. It can also be anticipated that the TP fluorophores may be applicable to quantification of macromolecules in gels or fluids.

Acknowledgements

The authors would like to thank Dr Fabrice Cordelières for his assistance regarding cellular imaging. This research was supported by a joint PhD fellowship from CNRS and the Institut Curie for B. D. This work has benefited from the facilities and expertise of the Small Molecule Mass Spectrometry platform of IMAGIF (Centre de Recherche de Gif – www.imagif.cnrs.fr).

Notes and references

1 W. R. Zipfel, R. M. Williams and W. W. Webb, *Nat. Biotechnol.*, 2003, **21**, 1369–1377.
2 B.-G. Wang, K. König and K.-J. Halbhuber, *J. Microsc.*, 2010, **238**, 1–20.
3 C. Xu, W. Zipfel, J. B. Shear, R. M. Williams and W. W. Webb, *Proc. Natl. Acad. Sci. U. S. A.*, 1996, **93**, 10763–10768.
4 C. Xu and W. W. Webb, *J. Opt. Soc. Am. B*, 1996, **13**, 481–491.
5 J. Zyss and I. Ledoux, *Chem. Rev.*, 1994, **94**, 77–105.
6 S.-J. Chung, K.-S. Kim, T.-C. Lin, G. S. He, J. Swiatkiewicz and P. N. Prasad, *J. Phys. Chem. B*, 1999, **103**, 10741–10745.
7 C. Katan, S. Tretiak, M. H. V. Werts, A. J. Bain, R. J. Marsh, N. Leonczek, N. Nicolaou, E. Badaeva, O. Mongin and M. Blanchard-Desce, *J. Phys. Chem. B*, 2007, **111**, 9468–9483.
8 C. Katan, M. Charlot, O. Mongin, C. Le Droumaguet, V. Jouikov, F. Terenziani, E. Badaeva, S. Tretiak and M. Blanchard-Desce, *J. Phys. Chem. B*, 2010, **114**, 3152–3169.
9 V. Parthasarathy, S. Fery-Forgues, E. Campioli, G. Recher, F. Terenziani and M. Blanchard-Desce, *Small*, 2011, **7**, 3219–3229.
10 M. Pawlicki, H. A. Collins, R. G. Denning and H. L. Anderson, *Angew. Chem., Int. Ed.*, 2009, **48**, 3244–3266.
11 L. Porrès, O. Mongin, C. Katan, M. Charlot, T. Pons, J. Mertz and M. Blanchard-Desce, *Org. Lett.*, 2004, **6**, 47–50.
12 M. Liang, W. Xu, F. Cai, P. Chen, B. Peng, J. Chen and Z. Li, *J. Phys. Chem. C*, 2007, **111**, 4465–4472.
13 C. D. Andrade, C. O. Yanez, M. a Qaddoura, X. Wang, C. L. Arnett, S. a Coombs, J. Yu, R. Bassiouni, M. V. Bondar and K. D. Belfield, *J. Fluoresc.*, 2011, **21**, 1223–1230.
14 T. Gallavardin, M. Maurin, S. Marotte, T. Simon, A.-M. Gabudean, Y. Bretonnière, M. Lindgren, F. Lerouge, P. L. Baldeck, O. Stéphan, Y. Leverrier, J. Marvel, S. Parola, O. Maury and C. Andraud, *Photochem. Photobiol. Sci.*, 2011, **10**, 1216–1225.
15 S. Luo, E. Zhang, Y. Su, T. Cheng and C. Shi, *Biomaterials*, 2011, **32**, 7127–7138.
16 P. S. Low and S. A. Kularatne, *Curr. Opin. Chem. Biol.*, 2009, **13**, 256–262.
17 K. Zelenka, L. Borsig and R. Alberto, *Bioconjugate Chem.*, 2011, **22**, 958–967.
18 C. Allain, F. Schmidt, R. Lartia, G. Bordeau, C. Fiorini-Debuisschert, F. Charra, P. Tauc and M.-P. Teulade-Fichou, *ChemBioChem*, 2007, **8**, 424–433.
19 C. Allain, M.-P. Teulade-Fichou, C. Fiorini-Debuisschert and F. Charra, WO2008/055969, 2008.
20 G. Metge, C. Fiorini-Debuisschert, F. Charra, G. Bordeau, E. Faurel and M. P. Teulade-Fichou, *Proc. SPIE*, 2010, 7715, 77150Q-77150Q-7.
21 B. Dumat, G. Bordeau, E. Faurel-Paul, F. Mahuteau-Betzer, N. Saettel, M. Bombled, G. Metgé, F. Charra, C. Fiorini-Debuisschert and M.-P. Teulade-Fichou, *Biochimie*, 2011, **93**, 1209–1218.
22 G. Bordeau, R. Lartia, G. Metge, C. Fiorini-Debuisschert, F. Charra and M.-P. Teulade-Fichou, *J. Am. Chem. Soc.*, 2008, **130**, 16836–16837.
23 C. Serbutoviez, J.-F. Nicoud, J. Fischer, I. Ledoux and J. Zyss, *Chem. Mater.*, 1994, **6**, 1358–1368.
24 C.-H. Yang, H.-L. Chen, Y.-Y. Chuang, C.-G. Wu, C.-P. Chen, S.-H. Liao and T.-L. Wang, *J. Power Sources*, 2009, **188**, 627–634.
25 R. Brodersen, *J. Biol. Chem.*, 1979, **254**, 2364–2369.
26 M. S. Baptista and G. L. Indig, *J. Phys. Chem. B*, 1998, **102**, 4678–4688.
27 V. S. Jisha, K. T. Arun, M. Hariharan and D. Ramaiah, *J. Am. Chem. Soc.*, 2006, **128**, 6024–6025.
28 E. A. Enyedy, L. Horváth, A. Hetényi, T. Tuccinardi, C. G. Hartinger, B. K. Keppler and T. Kiss, *Bioorg. Med. Chem.*, 2011, **19**, 4202–4210.
29 A. Baldridge, S. Feng, Y.-T. Chang and L. M. Tolbert, *ACS Comb. Sci.*, 2011, **13**, 214–217.
30 D. C. Carter and J. X. Ho, in *Advances in Protein Chemistry*, ed. V. N. Schumaker, Elsevier Academic Press, 1994, pp. 153–196.
31 G. Sudlow, D. J. Birkett and D. N. Wade, *Mol. Pharmacol.*, 1975, **11**, 824–832.
32 G. Sudlow, D. J. Birkett and D. N. Wade, *Mol. Pharmacol.*, 1976, **12**, 1052–1061.

33 T. Peters, *All About Albumin: Biochemistry, Genetics, and Medical Applications*, Elsevier Academic Press, 1996.
34 U. Kragh-Hansen, V. T. G. Chuang and M. Otagiri, *Biol. Pharm. Bull.*, 2002, **25**, 695–704.
35 T. Tomasic and L. P. Masic, *Curr. Med. Chem.*, 2009, **16**, 1596–1629.
36 A. Degterev, A. Lugovskoy, M. Cardone, B. Mulley, G. Wagner, T. Mitchison and J. Yuan, *Nat. Cell Biol.*, 2001, **3**, 173–182.
37 T. T. Talele, P. Arora, S. S. Kulkarni, M. R. Patel, S. Singh, M. Chudayeu and N. Kaushik-Basu, *Bioorg. Med. Chem.*, 2010, **18**, 4630–4638.
38 J. Dong, K. M. Solntsev, O. Poizat and L. M. Tolbert, *J. Am. Chem. Soc.*, 2007, **129**, 10084–10085.
39 D. Epps and T. Raub, *Anal. Biochem.*, 1995, **227**, 342–350.
40 R. M. Martin, H. Leonhardt and M. C. Cardoso, *Cytometry, Part A*, 2005, **67**, 45–52.